Symmetric Few-Mode Fiber Couplers as the Key Component for Broadband Mode Multiplexing

Christos P. Tsekrekos and Dimitris Syvridis

***Abstract*—All-fiber broadband mode multiplexers (MMUXs) for mode and wavelength division multiplexing transmission systems are designed and analyzed. The MMUXs are based on cascaded 2-D or 3-D symmetric few-mode fiber (FMF) couplers. The MMUXs are optimized for operation over the C band and multiplex modes LP_{01}, LP_{11a}, LP_{11b}, LP_{21a}, LP_{21b}, and LP_{02} with a nearly flat response and an average insertion loss around 1.6 dB, depending on the design approach. The operation of the FMF couplers and the MMUXs is analyzed numerically by means of a full-vectorial beam propagation method. If the two polarization states of each LP mode are further considered, such all-fiber MMUXs can be used to combine 12 spatial channels, supporting an order of magnitude capacity increase—compared to a single spatial channel system—in optical fiber transmission systems through space (mode and polarization) division multiplexing.**

***Index Terms*—Beam propagation method, few-mode fibers, mode division multiplexing, optical fiber couplers, optical fiber devices, wavelength division multiplexing.**

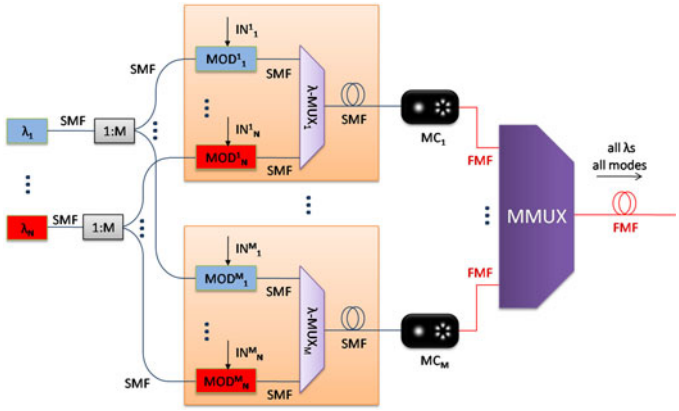

Fig. 1. Subsystem concept for the transmitting end of a FMF link that uses MDM and WDM. Broadband MCs and a broadband MMUX are required.

I. Introduction

THE need for higher capacity than what single-mode fiber (SMF) systems can support has turned research efforts to mode division multiplexing (MDM) over few-mode fibers (FMFs). Although system demonstrations have shown the feasibility of MDM for long-haul transmission [1], [2], the development of MDM components remains a major issue. It is important to note that MDM components should be compatible with other transmission techniques, especially wavelength division multiplexing (WDM), so that MDM over FMFs truly takes the optical capacity further than the SMF limits.

In relation to MDM, optical fiber couplers have been proposed for mode conversion and multiplexing [3]–[7]. The suitability of a mode multiplexer (MMUX) for use with several higher order modes is an important feature, since capacity increase is the motive behind MDM. At the same time, combining MDM with WDM dictates that a MMUX should operate over several tens of nanometers. Considerations for coupler-based MMUXs beyond LP_{01} and LP_{11} modes have been presented [6], [7], using asymmetric couplers that consist of a SMF and a FMF, with the effective index of the fundamental mode of the SMF designed to match the effective index of a certain higher order mode of the FMF. In this case, the asymmetric couplers perform simultaneously mode conversion and multiplexing. MMUXs based on asymmetric couplers can offer lossless mode coupling, i.e. a mode coupling efficiency of 100% for all modes, when the effective indices in each coupler perfectly match. However, index matching in such asymmetric couplers is wavelength dependent [5]–[7].

In this paper, mode coupling in symmetric FMF couplers, which consist of identical FMFs, is analyzed and all-fiber MMUXs are designed for WDM-MDM transmission systems utilizing modes LP_{01}, LP_{11a}, LP_{11b}, LP_{21a}, LP_{21b}, and LP_{02}. 2-D and 3-D couplers (this refers to whether the axes of the FMFs of a coupler are on a single plane or not) are considered, both yielding a similar performance of the MMUX. Such types of MMUXs can support a 12-spatial-channel system when polarization division multiplexing (PDM) is further considered. The use of symmetric couplers together with a proper design results in broadband MMUXs. The MMUXs are designed to be fully compatible with the transmission FMF. This is done by first choosing the transmission FMF (in our case a step-index FMF) and adapt the design to it. This assures compatibility of the MMUX with the transmission FMF and facilitates efficient coupling. Using symmetric couplers eliminates the need for accurate index matching required in asymmetric couplers, but presupposes separation of the mode conversion and multiplexing functions, as shown in Fig. 1. This means that broadband MCs are required [9].

First, the FMF under consideration is introduced and LP mode propagation is shortly described. Subsequently, coupling in symmetric FMF couplers is analyzed and the design and evaluation of MMUXs is presented. The results are obtained using a full-vectorial beam propagation method (BPM). This method makes no assumptions on the field distribution in the FMF

Manuscript received July 30, 2013; revised May 15, 2014; accepted May 23, 2014. Date of publication May 29, 2014; date of current version June 20, 2014.

The authors are with the Department of Informatics and Telecommunications, National and Kapodistrian University of Athens, 15784 Athens, Greece (e-mail: ctsekrekos@di.uoa.gr; dsyvridi@di.uoa.gr).

Color versions of one or more of the figures in this paper are available online at http://ieeexplore.ieee.org.

Digital Object Identifier 10.1109/JLT.2014.2327479

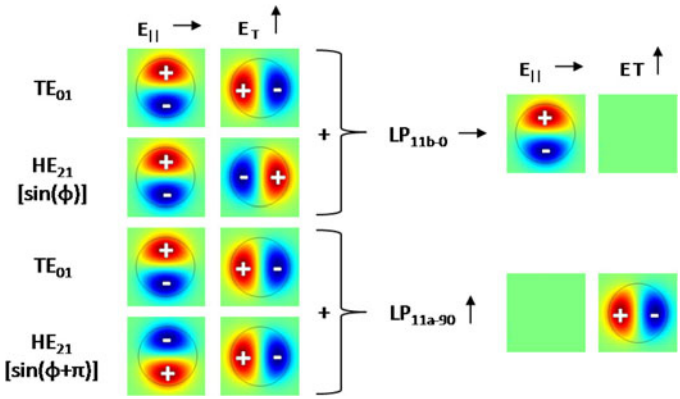

Fig. 2. Correspondence of modes LP_{11b-0}, LP_{11a-90} to the normal modes TE_{01} and HE_{21}. The transverse cartesian field components (horizontal $E_{\|}$ and vertical E_T) are shown to provide a straightforward illustration of the correspondence.

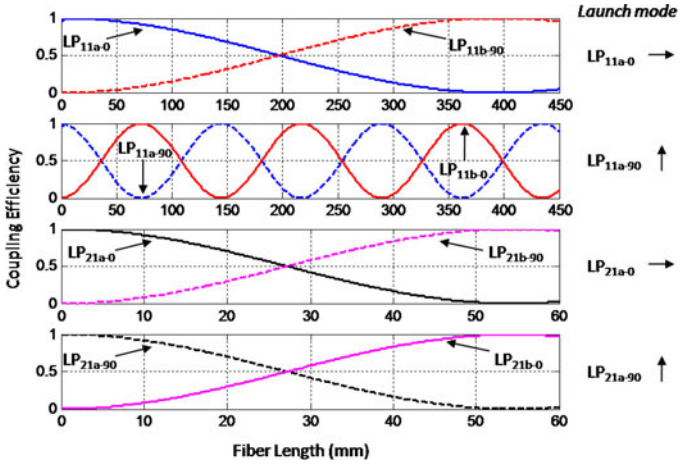

Fig. 3. Power interchange between degenerate states of modes LP_{11} and LP_{21} along propagation, at 1550 nm wavelength.

coupler, unlike the coupled-mode theory [8], and is therefore suitable for analyzing FMF couplers under different excitation and design conditions. The design of the MMUXs is aimed to approach an optimal performance over the *C* WDM band.

II. FMF and LP Modes

We consider a step-index FMF that supports modes LP_{01}, LP_{11}, LP_{21}, and LP_{02} within the wavelength range of 1373–1760 nm [9]. The core diameter is 13.5 μm and the refractive index at the cladding is given by [10]

$$n_{\text{cladding}} = \sqrt{1.3 + \frac{0.81996 \cdot \lambda^2}{\lambda^2 - 0.10396^2} - 0.01082 \cdot \lambda^2}$$

where λ is the free space wavelength in μm. The value of n_{cladding} at 1550 nm is 1.448334. The difference between the cladding and the core indices is taken to be 0.01 over the wavelength range considered.

LP modes are field distributions that arise when combining normal fiber modes with identical or very similar propagation coefficients. In this FMF, mode LP_{01} originates in normal mode HE_{11} (in both azimuthally degenerate states), mode LP_{11} in normal modes TE_{01}, TM_{01} and HE_{21}, mode LP_{21} in normal modes EH_{11} and HE_{31}, and mode LP_{02} in normal mode HE_{12}. As an example, the relation between modes LP_{11b-0}, LP_{11a-90} and the normal modes is illustrated in Fig. 2 (subscripts "0" and "90" indicate horizontal and vertical polarization, respectively).

Fig. 3 shows propagation of modes LP_{11} and LP_{21} at 1550 nm wavelength. Along the FMF, the power is monitored for both azimuthal degeneracies and polarizations. Power launched in LP_{11a-0} (LP_{11a-90}) will periodically couple to LP_{11b-90} (LP_{11b-0}) and vice versa. Similarly, power launched in LP_{21a-0} (LP_{21a-90}) will periodically couple to LP_{21b-90} (LP_{21b-0}) and vice versa. This is an intrinsic power interchange that expresses a periodical change in the relative phases of the normal modes and thus in the near-field pattern. The periodicity in the two top graphs of Fig. 3 is different, since modes LP_{11a-0} and LP_{11b-90} are a linear combination of modes TM_{01} and HE_{21}, whereas modes LP_{11a-90} and LP_{11b-0} are a linear combination of modes TE_{01} and HE_{21}, with modes TM_{01} and TE_{01} having different propagation coefficients. Propagation of modes LP_{01} and LP_{02} is not accompanied with changes of the near-field pattern, since each of these modes arises as the combination of the two azimuthally degenerate states of one normal mode that have the same propagation coefficient.

III. FMF Couplers

Optical fiber couplers have a wide range of applications in optical fiber communication systems. Both single-mode and multimode fiber (MMF) couplers are commercially available to be used as optical splitters/combiners. The criterion for fabricating these couplers is the ratio of optical power splitting. In the case of MMF couplers, the fabrication process does not deal with the distribution of power over the mode spectrum, but simply monitors the optical power under overfilled launch conditions. For FMF couplers, in the context of MDM, such an approach is not satisfactory, since the modal power distribution is a crucial feature. In this section, 2×2 FMF couplers are examined under excitation with individual FMF LP modes. The FMF considered is the one described in the previous section. The coupler is modeled as two parallel cylindrical waveguides of refractive index that corresponds to the index of the FMF core, the background index corresponding to the cladding index. This is a common way of modeling couplers, but it should be noted that the interaction lengths in this case correspond to the effective lengths of real couplers that have transition ends (the exact form of which depends on the fabrication technique) where fibers gradually approximate.

In a 2×2 fiber coupler, the optical power couples from one fiber core to the other periodically. In a coupler consisting of SMFs, the optical power propagates over the fundamental mode of each fiber. The maximum power coupling efficiency reaches 100% when the SMFs are identical, so that the effective indices of the fundamental modes of the two SMFs are equal. The larger the difference between these indices, the lower the maximum power coupling efficiency. The length over which the power

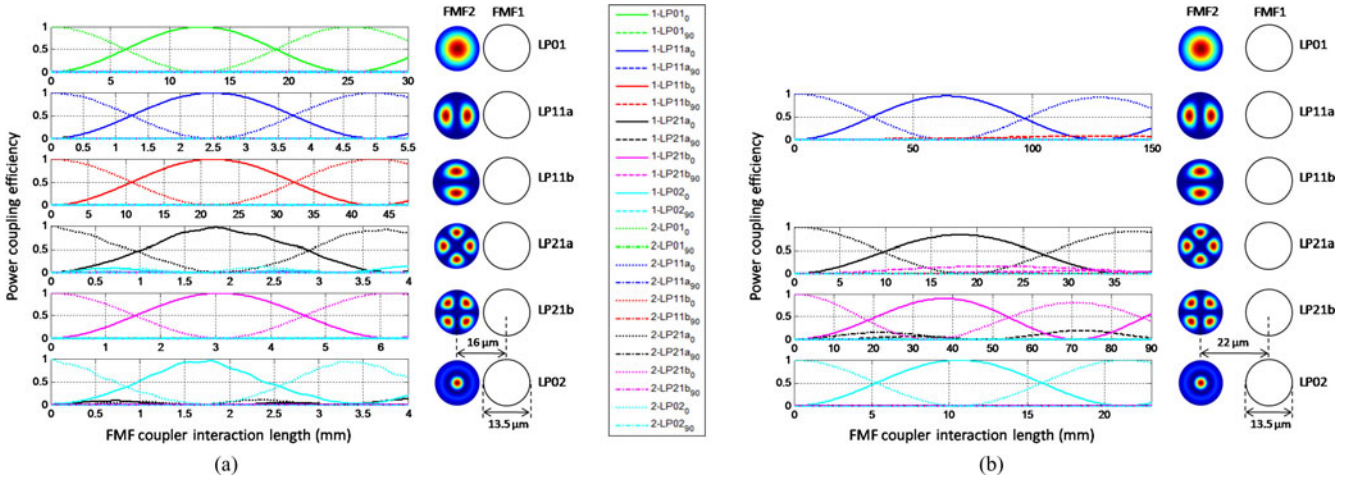

Fig. 4. Power coupling efficiency evolution along a FMF coupler for excitation of FMF2 with a single LP mode at 1550 nm, when the distance between the FMF cores is (a) 16 μm (b) 22 μm. The LP excitation modes are of horizontal polarization. Power is calculated using the overlap integral of the coupler field with the field of the individual FMF LP modes. The cases of modes LP_{01} and LP_{11b} are omitted in (b), since the FMF lengths required are very long.

coupling efficiency is first maximized is the coupling length (L_c). The value of L_c is wavelength dependent and further depends on the distance between the two fiber cores of the coupler.

The case of a coupler consisting of two identical FMFs involves a more complicated coupling process. In principle, power launched into a certain mode of one FMF of the coupler will not couple only to the same mode of the other FMF but to the other modes as well. The maximum power coupling efficiency between two modes reduces as the difference between their effective indices increases. Most of the power will be coupled to the same mode of the other FMF and a smaller portion will be coupled to the other modes. The maximum power coupling efficiency between two different modes also depends on the distance between the two FMF cores, reducing as the overlap of the two mode fields decreases [8]. It should be noted that by LP modes, the LP modes of the individual FMF are considered. This is because, the interest in the FMF coupler lies in its optical output, where the two FMFs are isolated. The LP modes of a single FMF are not modes of the coupler and, strictly speaking, especially when the distance between the two FMF cores of the coupler is small, the coupler modes cannot be considered as a combination of these LP modes. However, when the distance between the FMF cores of the coupler is large enough, the coupler modes can be fairly approximated as a combination of the modes of the individual FMF [8].

Fig. 4 shows the power coupling efficiency along the FMF coupler when one of the FMFs is excited by a certain LP mode at 1550 nm. The distance between the FMF cores was set at 16 μm and 22 μm to simulate two distinct cases. The distance of 16 μm corresponds to the case where the FMF cores are close enough so that coupling between different LP modes becomes observable. This is evident for modes LP_{21a} and LP_{02}. As it can be seen in Fig. 4(a), a portion of the power launched in mode LP_{21} (LP_{02}) is coupled to LP_{02} (LP_{21}). This inter-mode power exchange is because the effective indices of modes LP_{21} and LP_{02} are closer when compared to the ones of modes LP_{01} and LP_{11}. In particular, the mode indices of LP_{01}, LP_{11}, LP_{21}, and LP_{02} are 1.456558, 1.453908, 1.450602, and 1.449737, respectively, at 1550 nm. The same does not hold for LP_{21b}, since its evanescent field overlaps much less with the adjacent FMF.

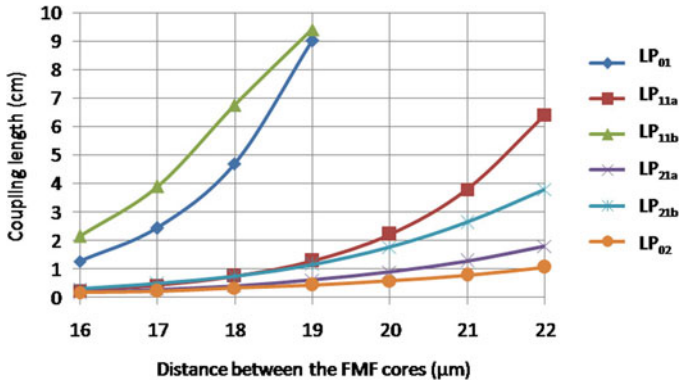

Fig. 5. Dependence of the coupling length on the distance between the two FMF cores of the symmetric coupler for all LP modes of the FMF, for horizontal polarization of the launched LP modes at 1550 nm.

On the contrary, the distance of 22 μm corresponds to the case where coupling between different LP modes is not evident and the L_c values are much larger. In particular, they are large enough so that power interchange between degenerate states of the launched LP mode in a single FMF core occurs in parallel to the power interchange between the two FMF cores. This is shown in Fig. 4(b) for modes LP_{11a}, LP_{21a}, and LP_{21b}. For mode LP_{02}, which corresponds to a single normal mode, power coupling follows the well-known sinus-square law as in a SMF coupler. The cases of modes LP_{01} and LP_{11b} are omitted in Fig. 4(b), since the coupler interaction lengths required are very large due to the increased L_c values. In particular, as the evanescent mode fields decay exponentially outside the core area, it is expected that L_c will tend to follow a similar exponential dependence. This is shown in Fig. 5 for lateral distance between

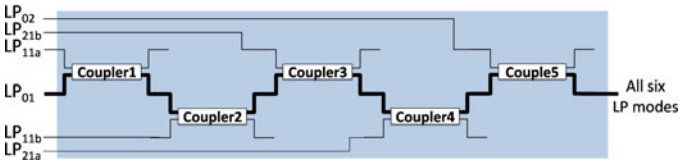

Fig. 6. The proposed MMUX based on cascaded 2-D FMF couplers. The central FMF path where modes gradually combine is indicated in bold.

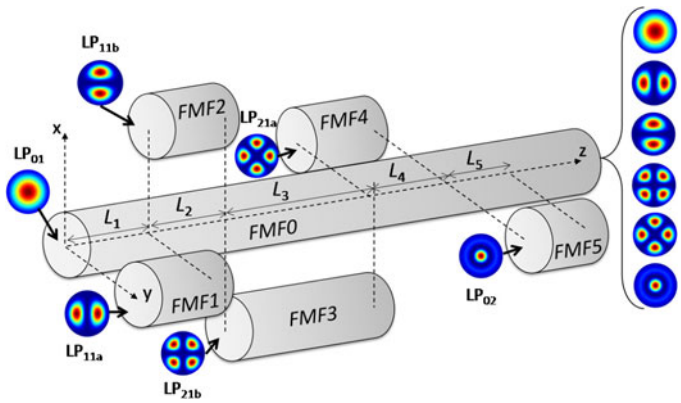

Fig. 7. A 3-D schematics of the structure used to simulate the MMUX based on cascaded 2-D couplers. The FMF cores are indicated as FMF0 to FMF5. Mode LP_{01}, LP_{11a}, LP_{11b}, LP_{21b}, LP_{21a}, and LP_{02} is launched at FMF0, FMF1, FMF2, FMF3, FMF4, and FMF5, respectively. All six LP modes are combined at the output of FMF0.

the FMF cores from 16 to 22 μm and for selective excitation with the FMF LP modes.

IV. MMUX Design and Performance

A. MMUX Based on Cascaded 2-D FMF Couplers

To combine the mode-channels in a MDM system, a MMUX is required. An all-fiber approach based on cascaded optical 2-D FMF couplers is presented and evaluated. 2-D couplers consist of parallel FMFs whose axes are on a single plane. Couplers consisting of two parallel FMFs are thus 2-D couplers. The MMUX is shown in Fig. 6. The first coupler is used to combine modes LP_{01} and LP_{11a}. Each coupler that follows combines another mode. The structure can also be viewed as comprising of a central FMF path where mode LP_{01} is initially launched and five cascaded couplers for combining modes LP_{11a}, LP_{11b}, LP_{21b}, LP_{21a}, and LP_{02}. The modes couple to the central FMF path in the order of descending L_c, the comparison holding for the same lateral distance between the FMF cores of the coupler (see the curve order in Fig. 5). This reduces the loss that a mode coupled into the central FMF path experiences when passing through the couplers that follow. The coupler interaction lengths are comparable to the L_c values to guarantee the broadband character of the device.

Fig. 7 shows a 3-D schematics of the structure used to simulate the proposed MMUX. Similarly to the previous section, each coupler is simulated as two parallel FMF cores. This

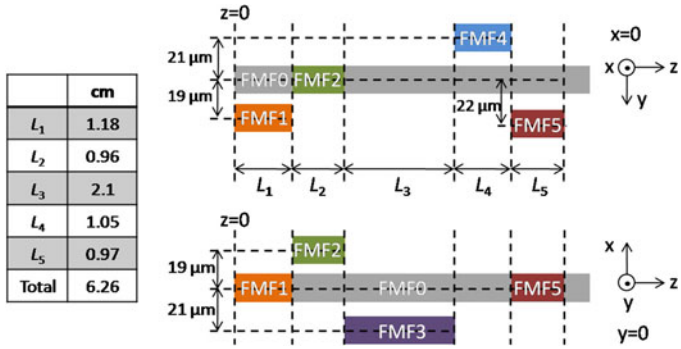

	cm
L_1	1.18
L_2	0.96
L_3	2.1
L_4	1.05
L_5	0.97
Total	6.26

Fig. 8. Schematic diagram of the simulation structure at planes $x = 0$ and $y = 0$. The distance between FMF cores and the interaction lengths of the couplers are shown.

effectively corresponds to having five FMF core segments, FMF1 to FMF5 corresponding to coupler 1 to 5, parallel to the central FMF core (FMF0) and in a sequential order along the direction of light propagation (z). Modes LP_{11a}, LP_{11b}, LP_{21b}, LP_{21a}, and LP_{02} are launched into FMF1, FMF2, FMF3, FMF4 and FMF5, respectively. The axes of FMF1, FMF4 and FMF5 are on the same plane, while the axes of FMF2 and FMF3 are on a perpendicular plane. The axis of FMF0 coincides with the intersection of these two planes. These perpendicular planes are used to optimize the MMUX performance (low and flattened insertion loss within the *C* band) that depends on the azimuthal orientation of the modes. It should be noted that although in Fig. 7 the FMF core segments are shown to be placed at 0°, 90°, 180° and 270° with respect to the *x*-axis, this is only the case for the simulation approach, so that the output field of each FMF core segment does not have any influence in the evaluation of the structure [it corresponds to a coupler output port not used (see Fig. 6)]. In practice, it is couplers 2 and 3 that are effectively on a plane perpendicular to that of couplers 1, 4 and 5.

The plane of each coupler and the orientation of modes LP_{11} and LP_{21} is chosen according to the L_c values and aiming at coupler interaction lengths reasonable for fabrication. Both LP_{11a} and LP_{11b} are launched with the lobe orientation that maximizes the overlap of the evanescent field with the adjacent FMF core. To achieve the 90° azimuthal shift in the relative orientation of modes LP_{11a} and LP_{11b} at the MMUX output, couplers 2 and 3 are on perpendicular planes. A similar approach was used in Ref. [5]. In contrast, while mode LP_{21a} is launched with an orientation that maximizes the portion of the evanescent field in the adjacent FMF core, mode LP_{21b} is launched so that this portion is minimized. Another approach is to set a 45° azimuthal shift to the plane of coupler 3 with respect to the plane of coupler 4, in order to maximize the overlap of the evanescent field with the adjacent FMF core in the case of LP_{21b} as well. However, this would increase the complexity of the design without introducing any significant advantage.

The goal of the MMUX design is to achieve a nearly flat response over the *C* band. The distance between FMF1, FMF2 and FMF0 is 19 μm, between FMF3, FMF4 and FMF0 21 μm and between FMF5 and FMF0 22 μm. Below 19 μm, the

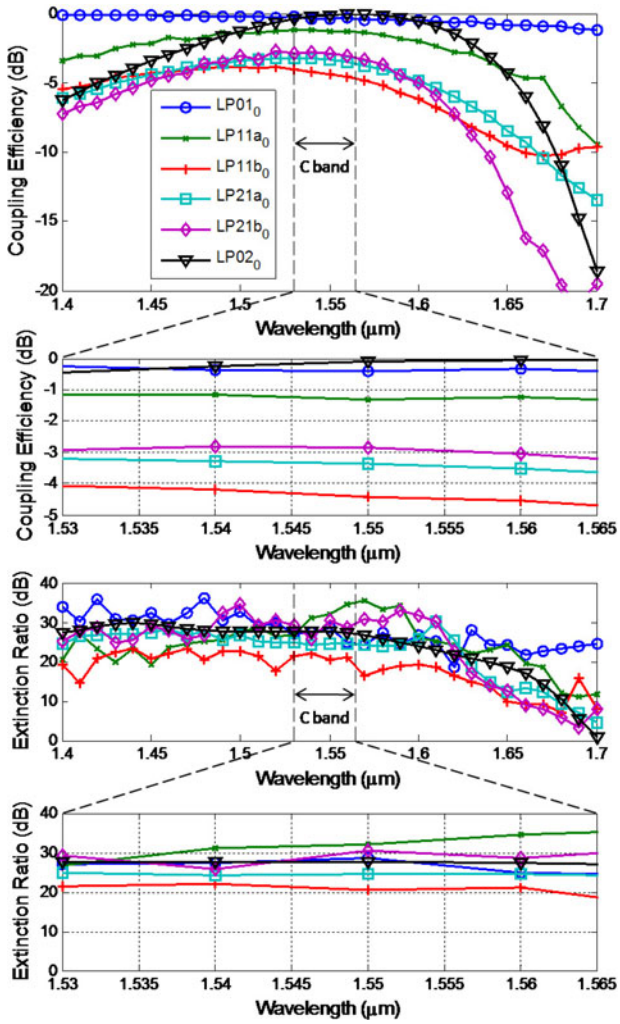

Fig. 9. Power coupling efficiency and extinction ratio of the 2-D-coupler based MMUX for each LP mode for horizontal polarization, i.e. the electric field is along the *y*-axis (see Fig. 7).

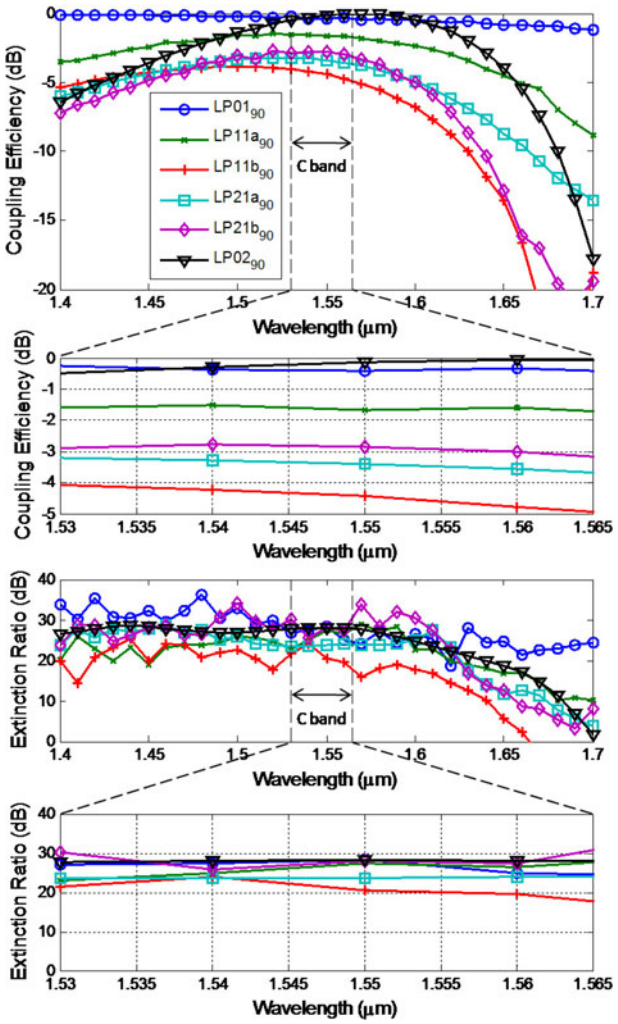

Fig. 10. Power coupling efficiency and extinction ratio of the 2-D-coupler based MMUX for each LP mode for vertical polarization, i.e. the electric field is along the *x*-axis (see Fig. 7).

L_c values become comparable for all modes, thus each coupling stage introduces similar loss for all modes, while beyond 22 μm, the L_c values, and consequently, the coupler interaction lengths, become very large (see Fig. 5). The interaction lengths of the couplers are chozen to be $L_1 = 1.18$, $L_2 = 0.96$, $L_3 = 2.1$, $L_4 = 1.05$, and $L_5 = 0.97$ cm. Fig. 8 shows the schematics of the simulation structure at planes $x = 0$ and $y = 0$ to further clarify the structure. The values of the interaction lengths of the couplers are smaller than the coupling length of the modes launched into them. This is to compensate for the coupling loss that the couplers introduce to the modes that pass through them and are already combined in previous coupling stages. Figs. 9 and 10 show the performance of the all-fiber MMUX over the wavelength range of 1.4 to 1.7 μm, as well as in more detail for the *C* band, for horizontal and vertical polarization of the launched LP modes, respectively.

The performance is evaluated in terms of mode power coupling efficiency and mode extinction ratio. The coupling efficiency, the opposite of which is the insertion loss due to the coupling mechanism, is defined as the ratio of the LP mode power at the output of FMF0 (including power coupled, simply due to propagation, to another degenerate state of the same LP mode, as described in Section II), where $z = L_1 + L_2 + L_3 + L_4 + L_5$, to the mode power at the launch plane of each mode, e.g. at $z = L_1 + L_2$ for the LP$_{21b}$ mode. The extinction ratio is used as a measure of the mode mixing that the MMUX introduces. It is calculated as the ratio of the LP mode power at the output of FMF0 (again including power coupled to another degenerate state of the same LP mode) to the total power of all other modes at the output of FMF0.

For horizontal polarization (see Fig. 9), within the *C* band, the average coupling efficiency of modes LP$_{01}$, LP$_{11a}$, LP$_{11b}$, LP$_{21a}$, LP$_{21b}$, LP$_{02}$ is -0.37, -1.26, -4.41, -3.42, -2.99, -0.17 dB, respectively, with an overall mean of -1.82 dB, while the difference between the maximum and minimum values of the coupling efficiency does not exceed 0.7 dB for all six LP modes. For the most part of the *C* band, for all modes, the ER does not fall below 20 dB. For vertical polarization, the results are similar (see Fig. 10). The main difference lies in the performance of the LP$_{11}$ modes. In particular, as it can

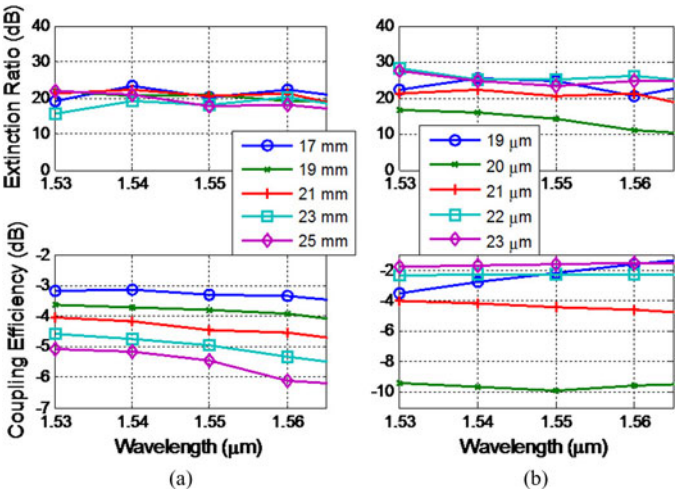

Fig. 11. MMUX performance for mode LP_{11b} for different values of (a) the FMF3 length (L_3) (b) the distance of FMF3 from FMF0.

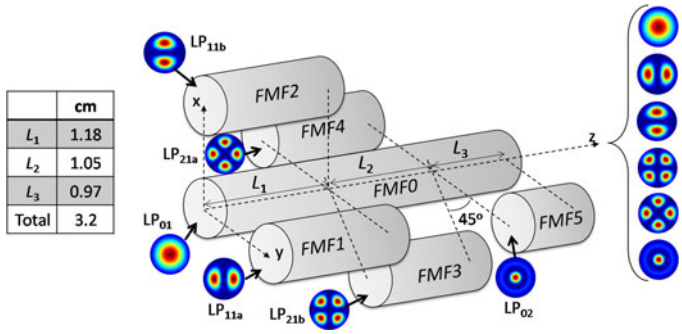

Fig. 12. A 3-D schematics of the structure used to simulate the MMUX based on cascaded 3-D couplers for simultaneously multiplexing the two azimuthal degenerate states of LP_{11} and LP_{21}. The FMF cores are indicated as FMF0 to FMF5. Mode LP_{01}, LP_{11a}, LP_{11b}, LP_{21b}, LP_{21a}, and LP_{02} is launch at FMF0, FMF1, FMF2, FMF3, FMF4, and FMF5, respectively. All six LP modes are combined at the output of FMF0.

be seen in Fig. 3, the period of the intrinsic LP_{11a} (LP_{11b}) mode coupling for horizontal polarization is about five times larger (smaller) than for the vertical one. This means that the coupling conditions in the coupling stages of the MMUX of the launched LP_{11-90} modes are different to those of the LP_{11-0} modes. However, the performance of the MMUX within the *C* band for vertical polarization is practically similar to that of horizontal polarization, with an overall mean coupling efficiency of -1.9 dB and a nearly flat response. Therefore, the proposed MMUX can be used with both polarization states.

It is interesting to consider the situation where the design parameters deviate from their selected values. The problem of the design of the proposed MMUX is an optimization problem that includes ten parameters. These parameters are the distances of FMF1 to FMF5 from FMF0 and the lengths of FMF1 to FMF5 (L_1 to L_5). Based on the results of Fig. 5, an estimation on the impact of deviations in the value of these parameters in the performance of the MMUX can be drawn. More specifically, though, in Fig. 11, a representative case is evaluated using the BPM. In particular, the performance of the MMUX for mode LP_{11b} is presented when the value of L_3 and the distance of FMF3 from FMF0 deviate from the values shown in Fig. 7. As it is expected, an increase (decrease) in the value of L_3—as long as it does not exceed the L_c value for mode LP_{11a}, results in a decrease (increase) in the overall coupling efficiency for mode LP_{11b} (as well as modes LP_{11a} and LP_{01}). The opposite will obviously hold for mode LP_{21b} that is launched in FMF3—as long as the L_3 value does not exceed the L_c value for mode LP_{21b}. Deviation in the value of the distance between FMF3 and FMF0 may be more critical. This is clearly evident when the distance between FMF3 and FMF0 is 20 μm. At this distance, the L_c value for mode LP_{11a} at 1550 nm is 2.2 cm, thus similar to the L_3 value (2.1 cm). This means that, taking into account the orientation in the proposed design, mode LP_{11b} will experience a very high loss when passing through coupler 3 of the MMUX. Therefore, in fabricating such a MMUX care should be taken primarily with respect to the distances between the FMF cores to avoid cases as the one shown in Fig. 11(b) for a distance of 20 μm.

In order to realize the proposed MMUX, the side-polishing technique could be used for the fabrication of the FMF couplers [11]. In the interconnection of the couplers care should be taken with the orientation of the mode profiles, similarly to the control of polarization that is required in polarization-dependent devices. A simple way to apply this control is through fiber rotation. This is a fundamental control function that will definitely be required in MDM subsystems. Furthermore, the fiber fusion technique has been proposed for fabricating FMF couplers [5], although it may not be possible to achieve a good level of geometric accuracy as with the side-polishing technique. In addition, the femtosecond direct laser writing technique has been used for the fabrication of SMF couplers [12], [13]. This is a very promising technique for the fabrication of 3-D optical waveguides and can be of immense importance for MDM components, as long as the index profile of the inscribed waveguides can be controlled to match that of the transmission FMF. It seems that for the time being this is not the case and further research is required [14].

B. MMUX Based on Cascaded 3D FMF Couplers

The previous design approach is based on cascaded 2-D FMF couplers, where at each stage another LP mode is added. Another approach can be followed, by considering 3-D FMF couplers. Such couplers consist of more than two parallel fibers, whose axes are not found on the same plane. 3-D couplers have recently been considered for application in MDM systems [6]. They have not been demonstrated experimentally, but they present an interesting paradigm for future MDM components. By considering 3-D FMF couplers, it is possible to design the MMUX as a cascade of three symmetric FMF couplers, the first two being 3-D ones comprising of three FMFs and the third one being a 2-D one, similarly to the previous approach. The 3-D schematics of this approach is shown in Fig. 12. The distances of the FMFs (1 to 5) to FMF0 are the same as in the 2-D-coupler approach. The values of the interaction lengths of the couplers are shown

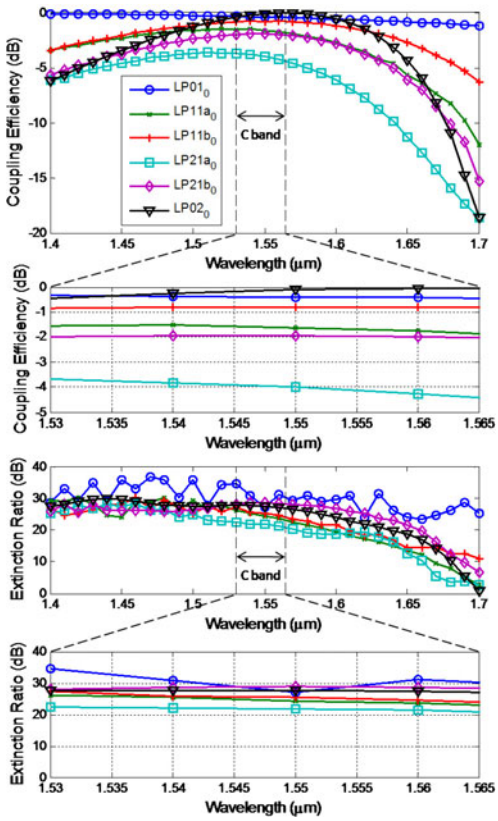

Fig. 13. Power coupling efficiency and extinction ratio of the 3-D-coupler based MMUX for each LP mode for horizontal polarization, i.e. the electric field is along the y-axis (see Fig. 12).

as an inset in Fig. 12 and are taken from the design of the 2-D-coupler approach. The difference of the 3-D-coupler approach to the 2-D-coupler approach is that FMF1 and FMF2 make a single 3-D FMF coupler with FMF0. The same holds for FMF3, FMF4 and FMF0. FMF5 and FMF0 form the same 2-D coupler as in the 2-D-coupler approach. In other words, the azimuthally degenerate states of the non-circularly symmetric modes LP_{11} and LP_{21} are combined in a single stage of the MMUX with symmetric 3D couplers. A geometric difference with the 2-D-coupler approach is that the plane defined by the axes of FMF0 and FMF3 forms a 45° angle with respect to the $x = 0$ plane, so that LP_{21a} and LP_{21b} require identical interaction lengths for being coupled with the same efficiency.

The results of the 3-D-coupler design approach are shown in Fig. 13 for the case of horizontal polarization of the launched LP mode fields. The performance is similar to the 2-D-coupler design approach. Within the C band, the coupling efficiency curves are nearly flat with an average value of -0.4, -1.69, -0.82, -4.07, -1.99, and -0.17 dB for modes LP_{01}, LP_{11a}, LP_{11b}, LP_{21a}, LP_{21b}, LP_{02}, respectively, yielding an overall average of -1.34 dB. The ER within the C band remains over 20 dB. The results for vertical polarization of the launched fields are practically the same and thus not shown. Due to the shorter total length of 3.2 cm, no differentiation appears in the case of the LP_{11} modes as in the 2-D-coupler approach.

V. Conclusion

The performance of symmetric FMF couplers was investigated under different launch conditions with individual FMF modes and different values of the distance between the two adjacent FMF cores, by means of a full-vectorial BPM. Based on this investigation, all-fiber MMUXs consisting of cascaded FMF couplers were designed and evaluated. The MMUXs combine modes LP_{01}, LP_{11a}, LP_{11b}, LP_{21a}, LP_{21b}, and LP_{02}. Two approaches were investigated. One that is based on five cascaded 2-D symmetric FMF couplers and one based on 3-D symmetric FMF couplers. In both cases, the proposed MMUXs perform similarly, achieving a nearly flat response for each mode within the C band and an average insertion loss about 1.6 dB, for both polarizations of the launched LP modes. The proposed MMUXs can be instrumental in applying MDM-PDM-WDM transmission.

References

[1] R. Ryf, S. Randel, A. H. Gnauck, C. Bolle, A. Sierra, S. Mumtaz, M. Esmaeelpour, E. C. Burrows, R. Essiambre, P. J. Winzer, D. W. Peckham, A. H. McCurdy, and R. Lingle, "Mode-division multiplexing over 96 km of few-mode fiber using coherent 6×6 MIMO processing," *J. Lightw. Technol.*, vol. 30, no. 4, pp. 521–531, Feb. 2012.

[2] M. Salsi, C. Koebele, D. Sperti, P. Tran, H. Mardoyan, P. Brindel, S. Bigo, A. Boutin, F. Verluise, P. Sillard, M. Astruc, L. Provost, and G. Charlet, "Mode-division multiplexing of 2×100 Gb/s channels using an LCOS-based spatial modulator," *J. Lightw. Technol.*, vol. 30, no. 4, pp. 618–623, Feb. 2012.

[3] N. Hanzawa *et al.*, "Demonstration of mode-division multiplexing transmission over 10 km two-mode fiber with mode coupler," presented at the Opt. Fiber Commun. Conf., Los Angeles, CA, USA, 2011, Paper OWA4.

[4] K. Y. Song, I. K. Hwang, S. H. Yun, and B. Y. Kim, "High performance fused-type mode-selective coupler using elliptical core two-mode fiber at 1550 nm," *Photon. Technol. Lett.*, vol. 14, no. 4, pp. 501–503, Apr. 2002.

[5] A. Li, X. Chen, A. Al Almin, and W. Shieh, "Fused fiber mode couplers for few-mode transmission," *Photon. Technol. Lett.*, vol. 24, no. 21, pp. 1953–1956, Nov. 2012.

[6] J. D. Love and N. Riesen, "Mode-selective couplers for few-mode optical fiber networks," *Opt. Lett.*, vol. 37, no. 19, pp. 3990–3992, Oct. 2012.

[7] B. Huang, C. Xia, G. Matz, N. Bai, and G. Li, "Structured directional coupler pair for multiplexing of degenerate modes," in *Proc. Opt. Fiber Commun. Conf.*, OSA Tech. Dig., 2013, Paper JW2A.25.

[8] K. Okamoto, *Fundamentals of Optical Waveguides.* New York, NY, USA: Elsevier, 2006.

[9] C. P. Tsekrekos and D. Syvridis, "All-fiber broadband LP_{02} mode converter for future wavelength and mode division multiplexing systems," *Photon. Technol. Lett.*, vol. 24, no. 18, pp. 1638–1641, Sep. 2012.

[10] C. M. Herzinger, B. Johs, W. A. McGahan, J. A. Woollam, and W. Paulson, "Ellipsometric determination of optical constants for silicon and thermally grown silicon dioxide via a multi-sample, multi-wavelength, multi-angle investigation," *J. Appl. Phys.*, vol. 83, no. 6, pp. 3323–3336, Mar. 1998.

[11] S.-M. Tseng and C.-L. Chen, "Side-polished fibers," *Appl. Opt.*, vol. 31, no. 18, pp. 3438–3447, Jun. 1992.

[12] K. Suzuki, V. Sharma, J. G. Fujimoto, E. P. Ippen, and Y. Nasu, "Characterization of symmetric [3 × 3] directional couplers fabricated by direct writing with a femtosecond laser oscillator," *Opt. Exp.*, vol. 14, no. 6, pp. 2335–2343, Mar. 2006.

[13] W.-J. Chen, S. M. Eaton, H. Zhang, and P. R. Herman, "Broadband directional couplers fabricated in bulk glass with high repetition rate femtosecond laser pulses," *Opt. Exp.*, vol. 16, no. 15, pp. 11470–11480, Jul. 2008.

[14] N. Jovanovic *et al.*, "Direct laser written multimode waveguides for astronomical applications," *Proc. SPIE*, vol. 7739, pp. 773923-1–773923-8, Jul. 2010.

Authors' biographies not available at the time of publication.